



**UNIVERSITY OF LEEDS**

This is a repository copy of *Sample preparation of anodised aluminium oxide coatings for scanning electron microscopy*.

White Rose Research Online URL for this paper:  
<http://eprints.whiterose.ac.uk/118199/>

Version: Accepted Version

---

**Article:**

Long, J, Borissova, A, Wilson, AD et al. (1 more author) (2017) Sample preparation of anodised aluminium oxide coatings for scanning electron microscopy. *Micron*, 101. pp. 87-94. ISSN 0968-4328

<https://doi.org/10.1016/j.micron.2017.06.010>

---

© 2017 Elsevier Ltd. This manuscript version is made available under the CC-BY-NC-ND 4.0 license <http://creativecommons.org/licenses/by-nc-nd/4.0/>

**Reuse**

Items deposited in White Rose Research Online are protected by copyright, with all rights reserved unless indicated otherwise. They may be downloaded and/or printed for private study, or other acts as permitted by national copyright laws. The publisher or other rights holders may allow further reproduction and re-use of the full text version. This is indicated by the licence information on the White Rose Research Online record for the item.

**Takedown**

If you consider content in White Rose Research Online to be in breach of UK law, please notify us by emailing [eprints@whiterose.ac.uk](mailto:eprints@whiterose.ac.uk) including the URL of the record and the reason for the withdrawal request.

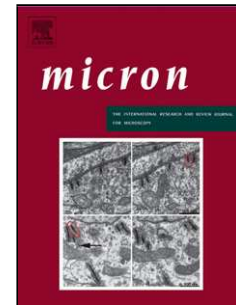


[eprints@whiterose.ac.uk](mailto:eprints@whiterose.ac.uk)  
<https://eprints.whiterose.ac.uk/>

## Accepted Manuscript

Title: Sample preparation of anodised aluminium oxide coatings for scanning electron microscopy

Authors: Jonathan Long, Antonia Borissova, Andrew David Wilson, Junia Cristina Avelar-Batista Wilson



PII: S0968-4328(17)30091-4  
DOI: <http://dx.doi.org/doi:10.1016/j.micron.2017.06.010>  
Reference: JMIC 2447

To appear in: *Micron*

Received date: 2-3-2017  
Revised date: 21-6-2017  
Accepted date: 21-6-2017

Please cite this article as: Long, Jonathan, Borissova, Antonia, Wilson, Andrew David, Avelar-Batista Wilson, Junia Cristina, Sample preparation of anodised aluminium oxide coatings for scanning electron microscopy. *Micron* <http://dx.doi.org/10.1016/j.micron.2017.06.010>

This is a PDF file of an unedited manuscript that has been accepted for publication. As a service to our customers we are providing this early version of the manuscript. The manuscript will undergo copyediting, typesetting, and review of the resulting proof before it is published in its final form. Please note that during the production process errors may be discovered which could affect the content, and all legal disclaimers that apply to the journal pertain.

# Sample Preparation of Anodised Aluminium Oxide Coatings for Scanning Electron Microscopy

Jonathan Long <sup>a</sup>, Antonia Borissova <sup>a</sup>, Andrew David Wilson <sup>b</sup>, Junia Cristina Avelar-Batista

Wilson <sup>b\*</sup>

<sup>a</sup> School of Chemical and Process Engineering, University of Leeds, Leeds LS2 9JT, UK

<sup>b</sup> BCW Treatments Ltd, 3C Innovation Drive, Bancroft Road, Burnley, Lancashire, BB10  
2FT, UK

\* Corresponding author

BCW Treatments Ltd, 3C Innovation Drive, Bancroft Road, Burnley, Lancashire, BB10 2FT,  
UK

Tel.: +44 (0) 1282 872484

Email: junia.wilson@bcw-treatments.co.uk

## Research Highlights

- Anodised aluminium oxide coating samples were prepared for SEM examination.
- Three preparation methods were trialled to assess coating thickness and structure.
- Cryogenic fracturing was found to be destructive to samples.
- Mechanical fracturing provided relatively accurate coating thickness measurements.
- Coating structure could only be evaluated from mechanically fractured samples.

**Abstract**

Characterisation of anodic aluminium oxide coatings and measurement of their thickness using microscopic techniques is valuable for analysing the effectiveness of the prior anodising process. Three different methods for preparing samples to view the coating cross-section (mechanical fracturing, cryogenic fracturing and metallography) were trialled and assessed for speed of implementation, simplicity and achievable measurement accuracy. Cryogenic fracturing was found to be destructive to samples. Mechanical fracturing yielded relatively accurate coating thickness measurements and coating structural information. Metallography provided the most accurate coating thickness measurement at the expense of coating structural information.

**Keywords:** Anodised aluminium oxide coatings; Scanning electron microscopy; Thickness measurements; Coating structure and morphology

**1. Introduction**

Pure metals corrode by reaction with oxygen and water in the environment causing detrimental changes to the properties of the material (ISO 8044:2015). Aluminium is highly reactive and quickly forms a protective natural oxide film in the presence of oxidants (Frank et al., 2000). This continuous coating across the aluminium surface provides corrosion resistance in oxidising environments. However, it is not sufficiently protective for typical industrial

applications and other corrosive environments where long-term performance is essential (Sheasby and Pinner, 2001).

Aluminium oxide coatings produced by anodising are comprised of a dielectric barrier layer at the substrate/oxide surface and a porous thick layer on the outermost surface. Aluminium alloys are anodised before application in automotive and construction industries to provide corrosion resistance. Anodic aluminium oxide has also received attention from nanomaterials and catalysis researchers due to the highly-ordered nanoporous structures achievable through anodising at relatively mild conditions (Sarkar et al., 2007; Poinern et al., 2011; O. Sanz et al., 2011; A. Belwalkar et al., 2008).

Depending on anodising conditions, anodic coatings can reach 150  $\mu\text{m}$  in thickness (A.M. Md Jani et al., 2013). Structural pores can be produced with diameters from 10 – 400 nm with an interpore spacing of 50–600 nm. Features at this scale can be characterised using scanning electron microscopy (SEM).

SEM analysis of metal oxide coatings is commonly carried out to characterise the morphology and structure of the coating, identify defects and contaminants present and to measure dimensions of features.

Careful preparation of specimens for SEM is crucial for achieving high quality images that are representative of the samples. Plan view images allow the surface morphology to be described and defects and contaminants to be identified. In order to directly measure the coating thickness, a cross-section image of the coating must be taken. Anodic aluminium oxide coatings are typically continuous on the surface of the aluminium substrate so the sample must be fractured to obtain a cross-section view image.

This paper assesses different sample preparation methods (mechanical fracturing, cryogenic fracturing and metallography (i.e. sectioning, mounting and polishing)) for viewing anodic coatings on aluminium using electron microscopy techniques. The objective is to identify a simple, reliable and fast preparation method for measuring anodic coating thicknesses and identifying microstructural features, thus saving time and improving efficiency for the academic research of anodic coatings.

## **2. Materials and Methods**

Aluminium alloy coupons of 4 different alloys were anodised in a conventional sulphuric acid batch anodising process at conditions that provided a coating thickness of 2–10  $\mu\text{m}$ . Coupons were 100 mm in length and 25 mm wide. The anodised alloys tested and their average thickness are given in Table 1. The identifiers in Table 1 were used for simple reference in this paper. Samples were imaged using scanning electron microscopy (SEM) in plan and cross-section views using a Carl Zeiss EVO MA15 scanning electron microscope at an accelerating voltage of 20kV. Energy Dispersive Spectroscopy (EDS) was also carried out for compositional analyses using an Oxford Instruments SDD detector and AZtec analysis software. For cross-section images, samples were prepared using three different methods and each method was analysed for repeatability, time efficiency and ability to produce samples that allowed accurate measurement of the coating thickness using SEM.

### **2.1. Plan view sample preparation**

Anodised coupons were protected with tissue paper, secured in a clamp and cut to approximate squares of 1 cm x 1 cm using a junior hacksaw. Samples were mounted on standard 12.5 mm specimen stubs using carbon adhesive stickers and carbon cement. The deposition of a conductive film was mandatory for SEM examination due to the insulating nature of aluminium oxide coatings. Therefore, samples were coated with 15 nm of iridium using an Agar high resolution sputter coater.

## **2.2. Cross-section view sample preparation**

Samples for SEM cross-section view imaging were prepared using three different methods: mechanical fracturing, cryogenic fracturing and metallography (i.e. sectioning, mounting and polishing). Regardless of the preparation method used, all specimens for cross-sectional imaging were also coated with iridium using an Agar high resolution sputter coater. Each cross-sectional method is described in detail below. In order to achieve accurate thickness measurements, the SEM scale bar was calibrated using a single crystal silicon specimen formed by electron beam lithography and marked with clearly visible squares of periodicity 10  $\mu\text{m}$  and dividing lines of 1.9  $\mu\text{m}$ .

### **2.2.1. Method 1: Mechanical fracturing**

Rectangular sections approximately 1 cm x 2 cm were sawn from coupons of each anodised alloy and notched as shown in Fig.1. Sections were protected with tissue paper, secured in a clamp and mechanically bent using a soft-head mallet towards the cut notch until the sample approximately formed a right angle. The sample was repositioned in the clamp according to Fig.1 and the clamp was gradually tightened until surface fractures were visible but before the sample was entirely snapped. The final angle varied depending on the alloy.

Samples were mounted to standard 32 mm specimen stubs using carbon adhesive and carbon cement with the fractured region facing vertically upwards.

### 2.2.2. Method 2: Cryogenic fracturing

Following the method originally described by Butler and Dawson (1976), a rectangular section approximately 1 cm x 2 cm was sawn from coupons of each anodised aluminium alloy. A notch was sawn into one face approximately half of the coupons thickness in depth, as shown in stage 1 of Fig.1. Sections were embrittled in liquid nitrogen for 10 minutes, then placed in a clamp and mechanically bent away from the notch and snapped into two pieces using a soft-head mallet.

Samples were mounted to standard 32 mm specimen stubs using carbon adhesive stickers and carbon cement with the cross-section of the sample coating facing vertically upwards.

### 2.2.3. Method 3: Metallography

Coupons of anodised aluminium alloys A and H were sectioned and cold mounted in Buehler's EpoxiCure 2 resin under vacuum. In order to ensure edge retention and protect the anodised layer, sectioned specimens were also wrapped in Al foil prior to cold mounting. Due to the non-conductive nature of the mounting resin, mounted specimens were also coated with a thin layer of iridium (conductive film) to avoid charging during SEM examination. In secondary electron (SE) imaging mode, no clear distinction between aluminium oxide coating and underlying aluminium alloy substrate could be made due to the successful metallographic preparation, which provided a perfectly flat and smooth cross-sectional surface. The lack of a topographical 'step' at the coating/substrate interface made both coating and substrate materials

indistinguishable in secondary electron imaging mode. Therefore, backscattered electron (BE) images were taken for mounted samples. In backscattered electron imaging mode a clear and distinguishable interface was visible between the coating and substrate, which allowed accurate coating thickness measurements to be taken. In order to perform coating thickness measurements in secondary electron imaging mode, chemical etching would be required to reveal the coating/substrate interface prior to the deposition of a conductive film to eliminate charging. Alternatively, conductive fillers could be added to Buehler's EpoxiCure 2 resin to solve charging issues during SEM examination. By doing so mounted samples would not need to be coated with a conductive film prior to SEM examination.

### 3. Results

#### **3.1. Sample Preparation**

All anodised alloys were successfully prepared for plan view imaging by the method described in section 2.1.

Fractures were created on the surfaces of anodised alloys F, M and H by mechanical fracturing as described in method 1. Anodised alloy A did not bend and fracture but snapped into two pieces. Examples of samples prepared by this method are shown in Fig.2. All anodised alloys were easily snapped after being immersed in liquid nitrogen as described in method 2, breaking at the notch.

All anodised alloys were successfully prepared using the metallographic method described in 2.2.3. Coating thickness was uniform and coating edges were damage-free, indicating that anodised layers were fully preserved.

### 3.2. Imaging

Plan view photomicrographs that allowed a description of the surface morphology and identification of defects and contaminants were taken for all anodised alloys. Coating surface features included surface imperfections (embedded particles, pores) grain boundary grooves (i.e. groove shaped imperfections along grain boundary regions formed due to preferential attack of grain boundaries) and etching pits. Etching pits are surface scallops or cavities formed as a consequence of different etching behaviours between intermetallic particles or inclusions and the aluminium matrix (Zhu et al., 2012; Ma et al., 2013). These features were significantly different for a particular aluminium alloy as depicted in Fig.3.

A significant quantity of embedded particles were found at the surface of the anodic film grown on alloy A (Fig.3a). Grain boundary grooves were clearly visible on the surface of the aluminium oxide coating grown on alloy F (Fig.3b). Anodic aluminium oxide coatings grown on alloys H (Fig.3c) and M (Fig.3d) exhibited a similar surface morphology characterised by surface scallops and pores.

Iron surface contaminants were also found on the surface of the aluminium oxide coating grown on alloy F (see Fig.4a). EDS mapping revealed that embedded particles at the surface of the aluminium oxide coating grown on alloy A were mainly silicon particles (Fig.4b).

Identifying and measuring the anodic coating with cross-section view photomicrographs was unsuccessful for samples prepared by cryogenic fracture. Viewing a section of the sample that showed the coating attached to the substrate at the correct angle for accurately measuring the coating thickness was extremely time consuming for all of the alloys examined.

For mechanically fractured samples, multiple consistent measurements of the coating thickness were taken by cross-section SEM photomicrographs on each alloy and were within the expected range for the anodising conditions used (see Table 3). Examples of cross-section photomicrographs taken of samples prepared by mechanical fracturing are given in Fig.5.

Multiple consistent coating thickness measurements were taken of samples which were metallographically prepared. In backscattered electron imaging mode, both coating cross-section and coating/substrate interface could be accurately determined. Sample preparation took longest by this method; however the coating was identified and measured most quickly.

Note that samples prepared by mechanical fracturing and by metallography (sectioning, mounting and polishing) were anodised at different experimental conditions, hence thickness measurements are not directly comparable. Nevertheless coating thickness measurements closely matched the expected range of 2-10  $\mu\text{m}$  which should have been achieved by the anodising process used in this investigation.

## **4. Discussion**

### **4.1. Plan view sample preparation**

Samples prepared for plan view images were largely successful. The coating and substrate structure were resilient to the high friction and vibration caused by sectioning with a junior hacksaw. However, the surface of alloy F was found to be contaminated with iron particles. This is likely due to breakage of the blade and insufficient cleaning before viewing.

A higher quality cutting device and more rigorous sample cleaning with a compressed air duster prior to coating and viewing would likely have mitigated this issue.

Silicon particles were successfully identified on the surface of anodised alloy A. Occlusion of silicon particles in anodic aluminium oxide films has been reported for films grown on aluminium alloys having a high silicon content (Fratila-Apachitei et al., 2004). This is the case for alloy A (A356), which has a nominal silicon content of 7 wt.%. These embedded particles are eutectic silicon particles which originated from the T6 heat treatment performed on alloy A (Wang, 2003; Merlin and Garagnani, 2009) and were not removed by alkaline etch and acid desmut processes that were carried out prior to sulphuric acid anodising. As a result silicon particles became incorporated to (i.e. trapped in) the aluminium oxide coating. During anodising the aluminium matrix is dissolved by the electrolyte to give rise to  $\text{Al}^{3+}$  ions which, by binding to oxygen, produce  $\text{Al}_2\text{O}_3$ . However, eutectic silicon particles present in the aluminium alloy undergo very slow oxidation and are incorporated in the anodic layer (Fratila-Apachitei et al., 2004). The oxidation of Si to give  $\text{SiO}_2$  is feasible but involves the application of considerable voltages, since the Si-O binding energy ( $466 \text{ kJmol}^{-1}$ ) is much higher than that of the Al-O ( $281 \text{ kJmol}^{-1}$ ); consequently silicon-containing species do not react and are retained within the anodic film as voltages applied during anodising are relatively low ( $\sim 20 - 25\text{V}$ ) (Ferlini et al., 2006).

The grain structure of aluminium oxide coatings grown on extruded alloy F (a 6xxx series alloy) had a similar structure to the alloys imaged by Zhu et al. (2012) and Ma et al. (2013), verifying the success of the sample preparation method used here for plan view SEM photomicrographs. The aluminium oxide coating grown on alloy H (5754) also exhibited a similar surface morphology (i.e. surface scallops) to anodic alumina films grown on the same

alloy (Aggerbeck et al., 2014), providing further validation to the plan-view sample preparation method used in this investigation.

#### **4.2. Cross-section view sample preparation**

Mechanically fractured samples revealed the cross-section of the coating allowing multiple, consistent measurements of coating thickness to be taken. Moreover, coating structure could be extracted from cross-sections of mechanically fractured samples as illustrated in Fig.5. Anodised aluminium oxide coatings grown on all four alloy types (Fig.5) exhibited a dense structure, which was achieved upon hydrothermal sealing of the coating after sulphuric acid anodising. The cylindrical pore structure characteristic of anodic alumina films was still visible at cross-sections of mechanically fractured samples despite the post-anodising hydrothermal sealing process.

Despite the inherent difficulties associated with samples fractured in this way, multiple consistent coating thickness measurements were made. Data presented in Table 3 clearly shows that thickness measurements were consistent for each aluminium alloy type. Small standard deviations (less than 5%) were obtained, confirming that viewing angles were similar and did not affect thickness measurements. The consistency between measurements at many different locations on a sample indicates the reliability of the method. However, angles close to  $90^\circ$  (i.e. perpendicular to the coating/substrate interface) were always pursued prior to coating thickness measurements in order to increase accuracy. As evidenced in Fig.5, thickness measurements were taken at similar angles and almost perpendicular to the coating cross-section. In order to achieve this, sample manipulation (e.g. tilting) was usually required.

Although thickness measurements were consistent, there is an associated inaccuracy with all measurements taken at any angle that is not completely perpendicular to the coating cross-section. As the viewing angle increases, so does the underestimation of the coating thickness. Therefore it is desirable to view the coating cross-section strictly perpendicularly.

A low-magnification view of a mechanically fractured coating for alloy M is shown in Fig.6a. This figure shows the way in which different segments of fractured coating tend to obscure the cross-section of other segments. This made it difficult to locate a region that could be viewed at a sufficiently perpendicular angle to provide an accurate thickness measurement and that showed the coating attached to the substrate. It was not possible to view the exposed coating cross-sections in the foreground for this sample due to the angle the sample was mounted and the tilt limitations of the SEM. An appropriate viewing angle for the exposed cross-sections may have been achieved by removing and remounting the sample. This would be time consuming and it is the intention of this paper to identify a method that eliminates the requirement for such trial and error-based work. Therefore, attention should be paid whilst selecting sample areas for cross-sectional examination in order to achieve a successful viewing angle. Areas of mechanically fractured samples in which different segments of the fractured coating tend to obscure the cross-section of other segments should be clearly avoided.

Entirely snapping a sample reveals the surface coating cross-section. Mounting a snapped sample correctly allows the coating to be viewed perpendicularly. Butler and Dawson (1976) described a method for cryogenically fracturing samples. By immersing in liquid nitrogen prior to snapping, the sample was sufficiently embrittled to allow the sample be easily snapped.

The preparation of samples by cryogenic fracturing proved unsuccessful. Liquid nitrogen caused brittle fracture of the samples that damaged the structure of the coating and detached it from the substrate in multiple locations. This made it prohibitively time consuming to identify a location for the accurate measurement of the anodic coating thickness. An SEM photomicrograph of anodised alloy A that was cryogenically fractured is shown in Fig.6b. From this figure, it is difficult to differentiate between the substrate and the coating and no accurate measurement of the coating thickness was achieved.

In this study, samples were immersed for 10 minutes, removed and then snapped sharply according to the method described in the literature (Butler and Dawson, 1976). It may be that the time of immersion was too long for the alloys used here and that less time would reduce the damage to the coating. Additionally, each alloy examined in this research had a different ductility. Therefore they likely required a different immersion time before they became sufficiently brittle to produce a clean edge from snapping.

Metallographic preparation of aluminium oxide coated-samples successfully revealed the anodic coating cross-section at a perpendicular angle to the coating/substrate interface. By using increasingly fine grinding and polishing steps, an exceptionally flat cross-section sample was produced. This allowed instant identification and measurement of the thickness of the anodic coatings using SEM imaging in backscattered electron mode (see Fig.7). A viewing angle directly perpendicular to the coating cross-section was achieved, which gave the most accurate measurement of the coating thickness out of the three sample preparation methods examined. However, the process of flattening the surface removed microstructural features that were viewed in fractured samples as shown in Fig.5 and in Fig.8 for segments of fractured coating on alloy A prepared by mechanical fracturing. These photomicrographs (Fig.5 and

Fig.8) contain three-dimensional features that reveal microstructural properties that are not seen in Fig.7. It is also clear that coating microstructural features seen in Fig.5 are removed by metallographic preparation (see Fig.7e). Consequently, coating structure cannot be revealed by metallographic preparation, although thickness measurements are very accurate due to the perpendicular angle to the coating/substrate interface. Additionally, metallographic preparation requires specialist equipment, knowledge and considerably longer preparation times than fracturing methods.

Note that the thickness of aluminium oxide coatings on both alloy A and alloy H is slightly under 2  $\mu\text{m}$  (Figs. 7b and 7d) and is not directly comparable to those of samples prepared by mechanical bending (Fig.5). In the former samples a very low current density was used during anodising to significantly reduce the anodic film thickness. Therefore, metallographic preparation was proven to be a successful and accurate method to measure the thickness of brittle anodic films, especially if they are thin (i.e.  $< 2 \mu\text{m}$ ).

## 5. Conclusions

Mechanical fracturing was found to be fast and simple to implement with few tools required. There is an inherent inaccuracy associated with being unable to view the coating cross-section perpendicularly. This inaccuracy may become more critical for determining the coating thickness of thin (i.e.  $< 2 \mu\text{m}$ ) anodic aluminium oxide films. However, for many applications the accuracy will be sufficient provided that samples are manipulated to yield a viewing angle which is almost perpendicular to the cross-section. This method also reveals structural information about the coating and substrate, which is valuable for characterising the microstructure. Cast alloys will snap using this method due to their low ductility making identifying and measuring the coating a more time consuming process.

Cryogenic fracturing was found to be ineffective by the method investigated here. Immersing samples in liquid nitrogen for 10 minutes caused too much damage to the sample upon snapping. The coating could not be differentiated from the substrate for an accurate thickness measurement to be taken.

Metallographic preparation allowed for the most accurate coating thickness measurement to be taken at the expense of coating cross-sectional structure/morphology. The process of fine grinding and polishing flattens any coating microstructural features; consequently any morphological information regarding coating structure is 'lost'. Moreover, metallographic preparation requires specialist equipment and knowledge in addition to a considerably long preparation time.

The method of sample preparation should be selected based on the information required from imaging. Metallographic preparation provides the most accurate measurement of coating thickness, especially if anodic films are particularly thin ( $< 2 \mu\text{m}$ ). Mechanical fracturing

allows the cross-sectional microstructure of anodic coatings to be ascertained and provides sufficiently accurate coating thickness measurements for many applications. This method was found to be the most versatile among all trialled as coating microstructure and thickness could be simultaneously extracted from cross-sections. However, an appropriate viewing angle (i.e. almost perpendicular to the coating/substrate interface) for exposed cross-sections must be achieved for accuracy of thickness measurements. This may require substantial sample manipulation (i.e. samples may need to be removed and remounted several times in conjunction with tilting).

### **Acknowledgements**

The authors would like to thank the Regional Growth Fund (RGF) for financial support received from Project/Programme Reference No 01.09.07.01/2584C. They are also greatly indebted to Mr Stuart Mickelthwaite of Leeds Electron Microscopy and Spectroscopy for his much-valued assistance with SEM and to Buehler for their expertise and assistance with metallographic preparation.

### **References**

Aggerbeck, M., Canulescu, S., Dirscherl, K., Johansen, V.E., Engberg, S. Schou, J., Ambat, R., 2014. Appearance of anodised aluminium: Effect of alloy composition and prior surface finish, *Surface and Coatings Technology* 254 28–41.

- Belwalkar, A., Grasing, E., Van Geertruyden, W., Huang, Z., Misiolek, W.Z., 2008. Effect of Processing Parameters on Pore Structure and Thickness of Anodic Aluminum Oxide (AAO) Tubular Membranes. *Journal of Membrane Science* 319 (1-2) 192-198.
- Butler, W.O., Dawson, I.J., 1976. Application of cryogenic fracturing to the study of the cross-sectional structures of surface layers on metals. *Micron* (1969) 7 (2), 109-114.
- Ferlini, S., Costa, E., Ferri, E., 2006. Effetti del silicio nell'anodizzazione di leghe di alluminio (in Italian), *La Metallurgia Italiana* 9 60-62.
- Frank, W.B., Haupin, W.E., Dawless, R.K., Granger, D.A., Wei, M.W., Calhoun, K.J., Bonney, T.B., 2000. Aluminum, in: *Ullmann's Encyclopedia of Industrial Chemistry*. Wiley-VCH Verlag GmbH & Co. KGaA.
- Fratila-Apachitei, L.E., Tichelaar, F.D., Thompson, G.E., Terryn, H., Skeldon, P., Duszczyk, J., Katgerman L., 2004. A transmission electron microscopy study of hard anodic oxide layers on AlSi(Cu) alloys, *Electrochimica Acta* 49 3169–3177.
- ISO 8044:2015. Corrosion of metals and alloys. International Organization for Standardization, Geneva, Switzerland.
- Ma, Y., Zhou, X., Thompson, G.E., Nilsson, J.-O., Gustavsson, M., Crispin, A., 2013. Origin of streaks on anodised aluminium alloy extrusions. *Transactions of the IMF* 91 (1) 11-16.
- Md Jani, A.M., Losic D., Voelcker, N.H., 2013. Nanoporous anodic aluminium oxide: Advances in surface engineering and emerging applications. *Progress in Materials Science* 58 (5), 636-704.
- Merlin, M., Garagnani, G.L., 2009. Mechanical and microstructural characterisation of A356 castings realised with full and empty cores, *Metallurgical Science and Technology* 27 21-30.

- Poinern, G.E.J., Ali, N. Fawcett, D., 2011. Progress in Nano-Engineered Anodic Aluminum Oxide Membrane Development. *Materials* 4 (3), 487-526.
- Sanz, O., Echave, F.J., Odriozola, J.A., Montes, M., 2011. Aluminum Anodization in Oxalic Acid: Controlling the Texture of Al<sub>2</sub>O<sub>3</sub>/Al Monoliths for Catalytic Applications. *Industrial & Engineering Chemistry Research* 50 (4), 2117-2125.
- Sarkar, J., Khan, G.G., Basumallick, A., 2007. Nanowires: properties, applications and synthesis via porous anodic aluminium oxide template. *Bulletin of Materials Science* 30 (3), 271-290.
- Sheasby, P.G., Pinner, R., 2001. The surface treatment and finishing of aluminium and its alloy, sixth ed. ASM International, Ohio.
- Wang, Q.G., 2003. Microstructural effects on the tensile and fracture behaviour of aluminium casting alloys A356/A357, *Metallurgical and Materials Transactions A* 34 2887-2899.
- Zhu, H., Couper, M.J., Dahle, A.K., 2012. Effect of Process Variables on the Formation of Streak Defects on Anodized Aluminum Extrusions: An Overview. *High Temp. Mater. Proc.* 31, 105–111.

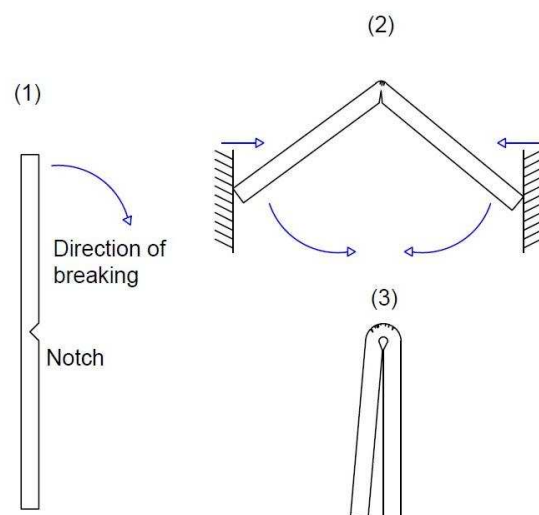


Fig.1: Mechanical fracturing method stages.



Fig.2: Samples prepared for SEM by mechanical fracturing for anodised alloys (a) M, (b) H, (c) F and (d) A.

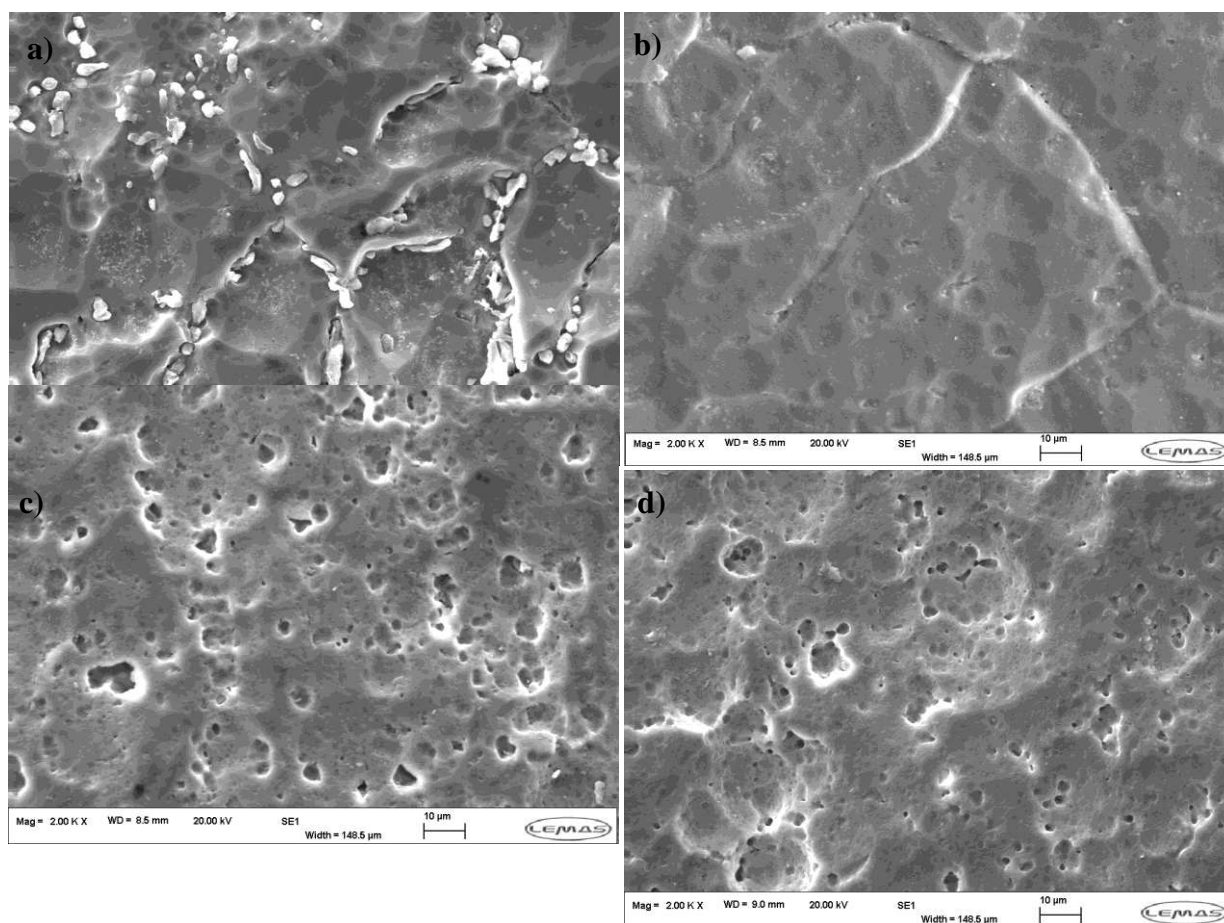


Fig.3: SEM plan view photomicrographs for anodised alloys (a) A, (b) F, (c) H and (d) M.

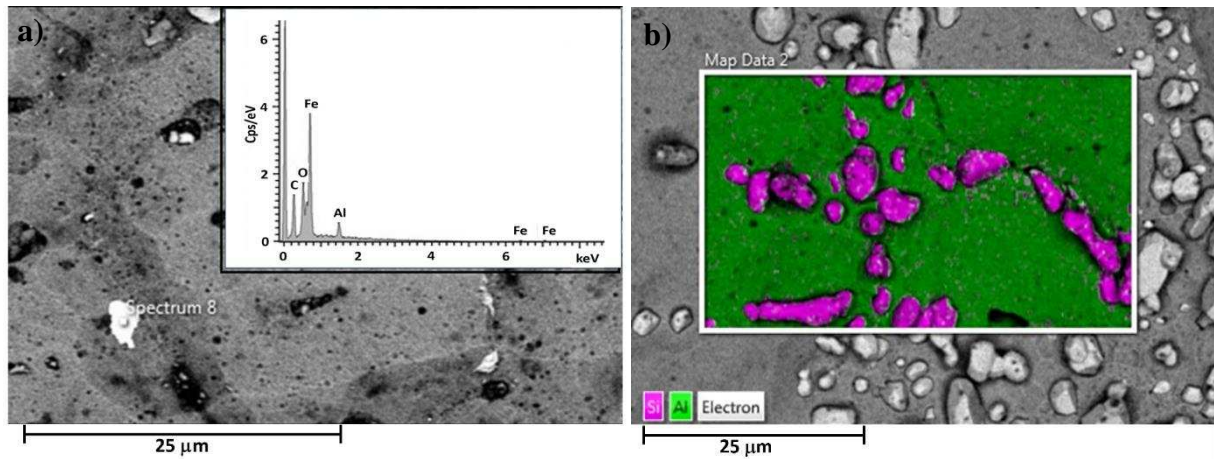


Fig.4: (a) Anodised alloy F with iron surface contaminant identified by EDS spot analysis and (b) anodised alloy A with silicon particles identified by EDS mapping.

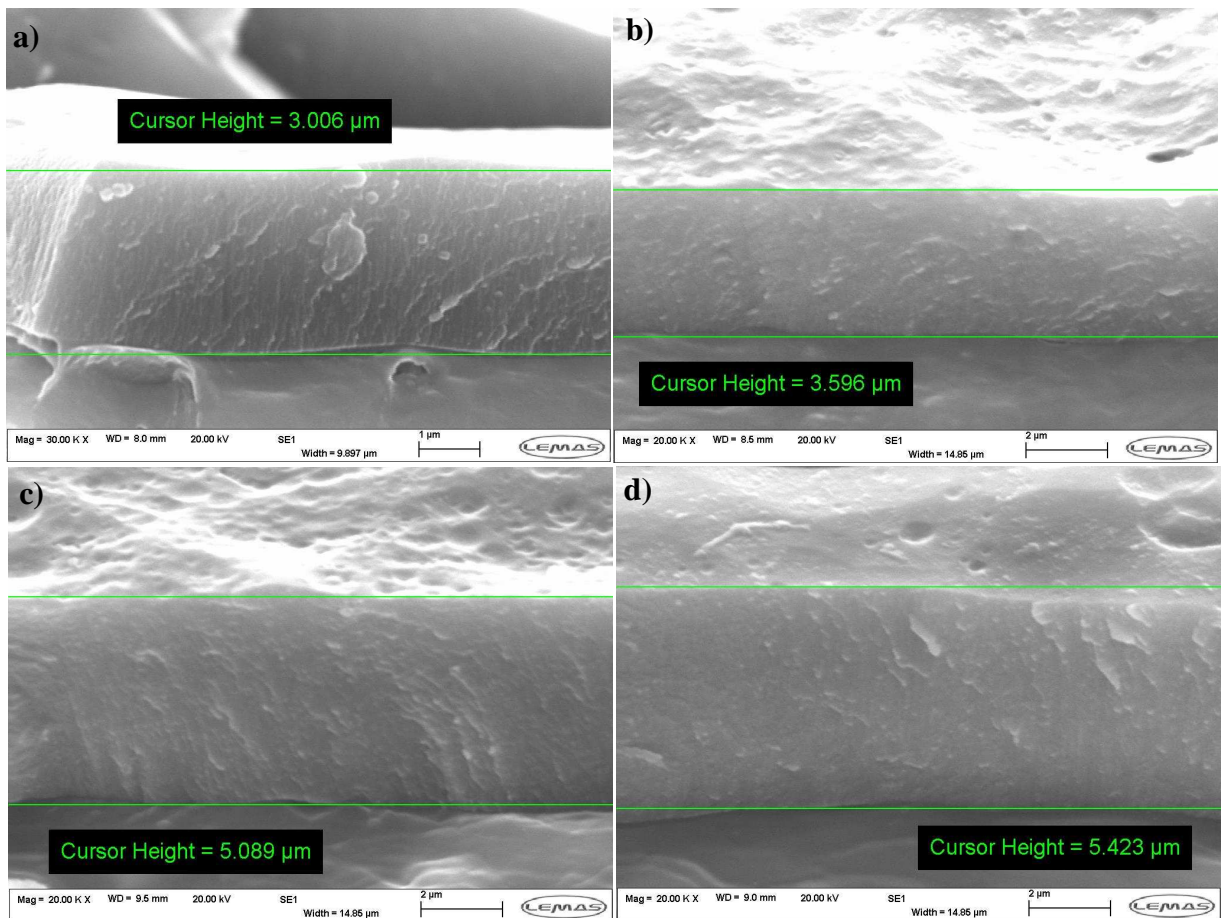


Fig.5: Cross-sectional SEM photomicrographs of anodised alloys (a) A, (b) F, (c) H and (d) M prepared by mechanical fracturing.

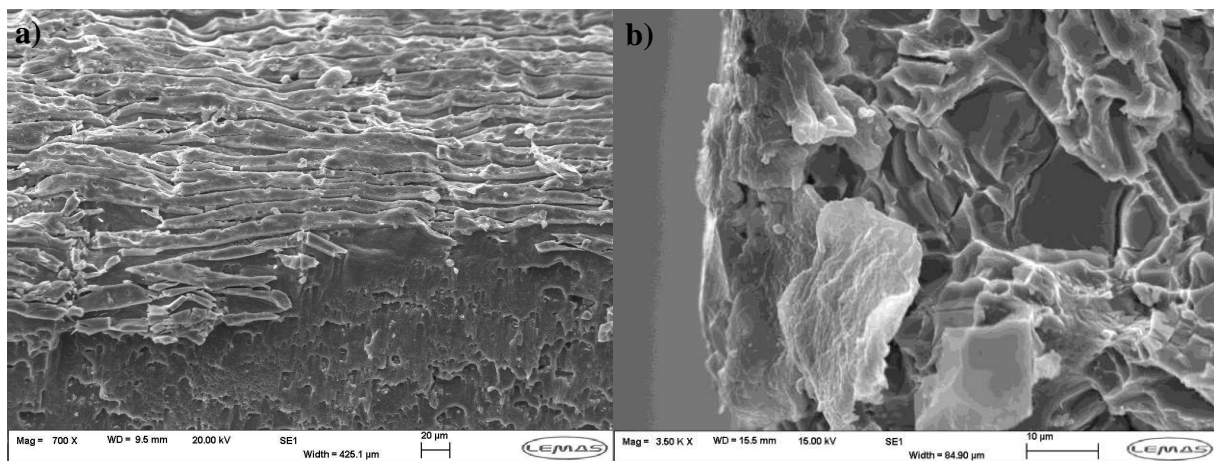


Fig. 6: (a) Low magnification SEM photomicrograph of the anodic aluminium oxide coating grown on alloy M fractured by mechanical bending and (b) SEM photomicrograph of anodised alloy A cryogenically fractured.

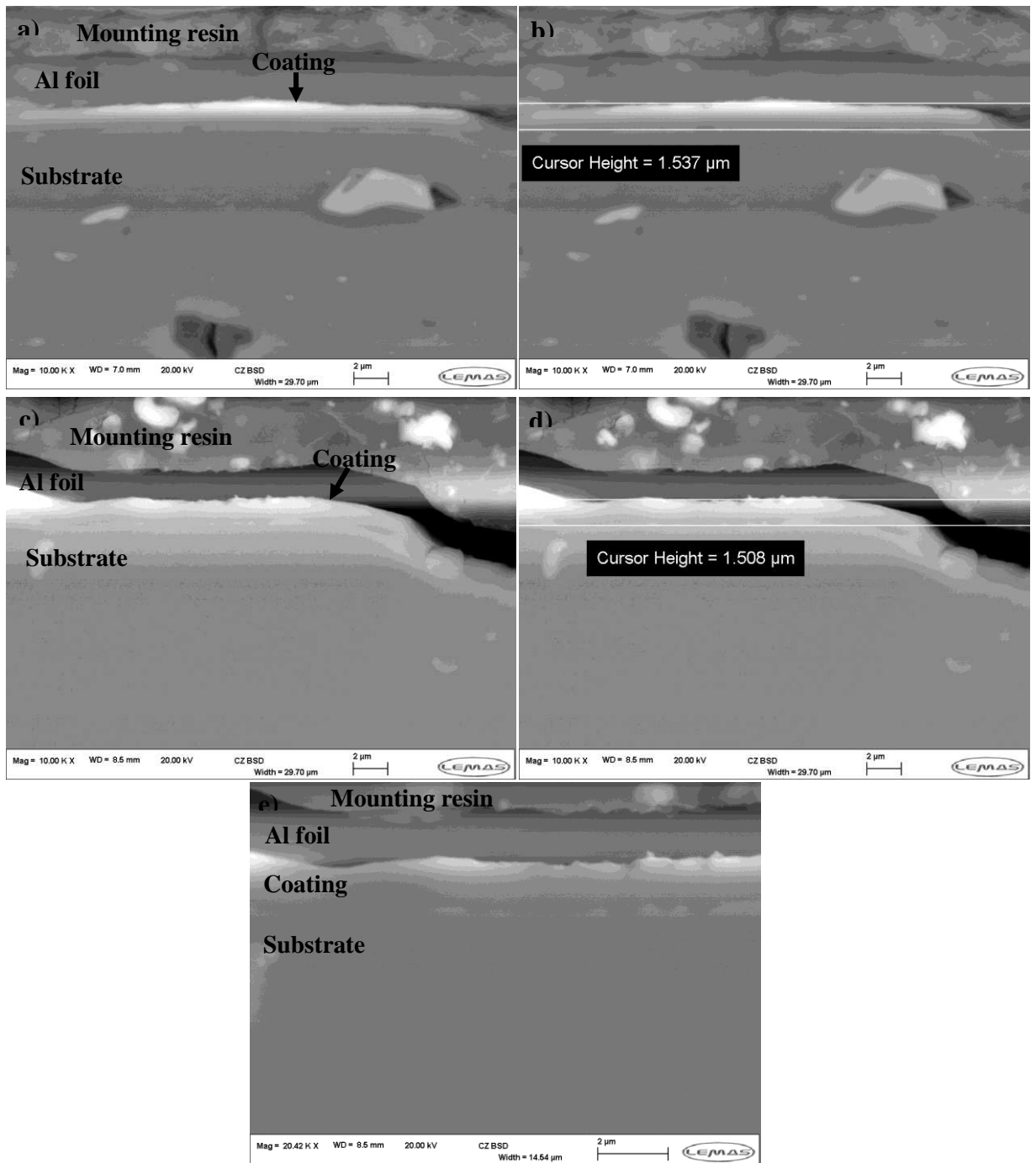


Fig.7: SEM photomicrographs of metallographically prepared specimens of (a) anodised alloy A, (b) anodised alloy A showing thickness measurement taken, (c) anodised alloy H, (d) anodised alloy H showing thickness measurement taken and (e) anodised alloy H at a comparable magnification of samples prepared by mechanical fracturing as in Fig.5.

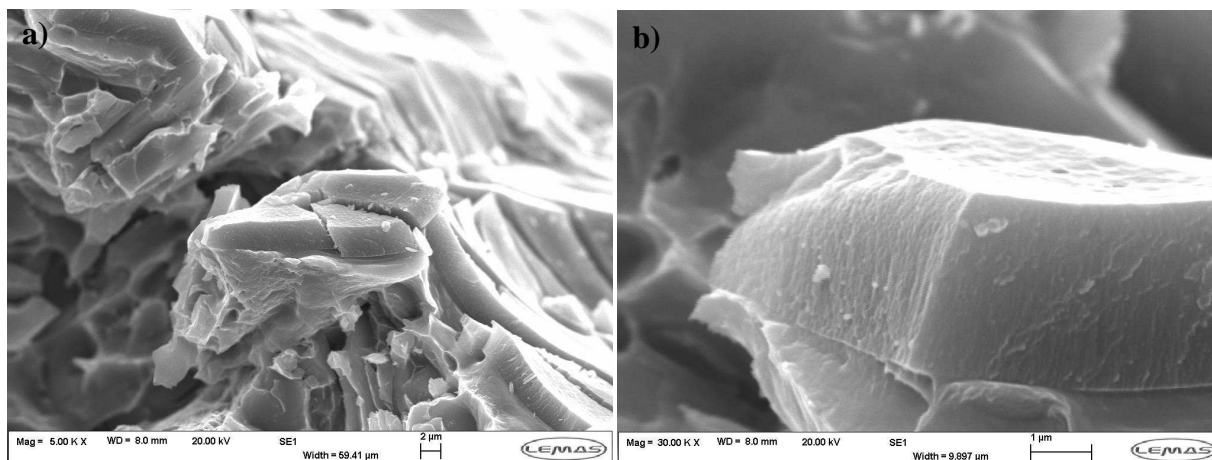


Fig.8: (a) SEM photomicrograph of anodised alloy A after mechanical fracturing. Three-dimensional microstructural features in these photomicrographs are not visible in samples which were metallographically prepared (Fig.7). (b) SEM photomicrograph showing a segment of anodised alloy A after mechanical fracturing, which allowed coating thickness measurements to be taken. Sample manipulation (tilting) was further required to achieve viewing angles which were almost perpendicular to the cross-section as shown in Fig.5a for this alloy.

Table 1: Anodised alloy types examined.

<b>Alloy</b>	<b>Temper / Heat Treatment</b>	<b>Type</b>	<b>Identifier</b>	<b>Coupon Thickness (mm)</b>
A356	T6	Casting	A	4.0
5754	H22	Sheet	H	1.4
6060	T6	Extrusion	F	2.0
5083	H111	Sheet	M	1.9

Table 2: Five-stage grinding and preparation method for preparing aluminium alloys for viewing anodised coating cross-sections. Preparation materials and methodology provided by Buehler.

<b>Base Surface</b>	<b>Size and Abrasive</b>	<b>Load (N) /Specimen</b>	<b>Base Speed (RPM)</b>	<b>Relative Rotation<sup>b</sup></b>	<b>Time (mins)</b>
CarbiMet	P400 Grit SiC, water cooled	22	300	>>	Until plane
TexMet C	9 $\mu\text{m}$ MetaDi Supreme Diamond <sup>a</sup>	22	150	<<	5
VerduTex	3 $\mu\text{m}$ MetaDi Supreme Diamond <sup>a</sup>	22	150	>>	4
VerduTex	1 $\mu\text{m}$ MetaDi Supreme Diamond <sup>a</sup>	22	150	>>	2
ChemoMet	0.02 $\mu\text{m}$ MasterMet 2 Colloidal Silica	22	150	<<	2

<sup>a</sup> MetaDi fluid extender as desired.

<sup>b</sup> Relative rotation key: >> Platen and specimen holder rotate in the same direction; << Platen and specimen holder rotate in opposite directions.

Table 3: Coating thicknesses measured using cross-sectional SEM photomicrographs with samples prepared by mechanical fracturing. Respective average thickness values from the five samples for each alloy and standard deviations are also shown.<sup>a</sup>

Alloy type	Thickness, $t$ ( $\mu\text{m}$ )					Average	Standard deviation
	$t_1$	$t_2$	$t_3$	$t_4$	$t_5$		
A	3.0	3.0	3.1	3.0	2.9	3.0	0.1
F	3.5	3.6	3.5	3.9	3.8	3.7	0.2
H	4.5	5.1	4.6	4.9	4.6	4.8	0.2
M	5.5	5.4	6.0	6.0	6.0	5.8	0.3

<sup>a</sup> All thickness measurements were taken from cross-sections examined at viewing angles almost perpendicular to the coating/substrate interface to minimise errors and increase accuracy.